

20 mA bidirectional laser triggering in planar devices based on vanadium dioxide thin films using CO₂ laser

Jihoon Kim,¹ Songhyun Jo,² Kyongsoo Park,² Ha-Joo Song,³ Hyun-Tak Kim,⁴ Bong-Jun Kim,⁵ and Yong Wook Lee^{1,2,*}

¹School of Electrical Engineering, Pukyong National University, 45 Yongso-ro, Nam-gu, Busan 608-737, South Korea

²Interdisciplinary Program of Biomedical, Mechanical & Electrical Engineering, Pukyong National University, 45 Yongso-ro, Nam-gu, Busan 608-737, South Korea

³Department of IT Convergence and Application Engineering, Pukyong National University, 45 Yongso-ro, Nam-gu, Busan 608-737, South Korea

⁴Metal-Insulator Transition Creative Research Center, Electronics and Telecommunications Research Institute, 218 Gajeong-ro, Yuseong-gu, Daejeon 305-700, South Korea

⁵Mobrik Co. Ltd., Yuseong-gu, Daejeon 305-700, South Korea
*yongwook@pknu.ac.kr

Abstract: By utilizing a CO₂ laser centered at ~10.6 μm as an optical stimulus, we demonstrated bidirectional laser triggering in a two-terminal planar device based on a highly resistive vanadium dioxide (VO₂) thin film. The break-over voltage of the VO₂-based device was measured as large as ~294.8 V, which resulted from the high resistivity of insulating VO₂ grains comprising the thin film and the large electrode separation of the device. The bidirectional current switching of up to 20 mA was achieved by harnessing the dramatic resistance variation of the device photo-thermally induced by the laser illumination. The transient responses of laser-triggered currents were also analyzed when laser pulses excited the device at a variety of pulse widths and repetition rates. In the transient responses, a maximum switching contrast between off- and on-state currents was measured as ~7067 with an off-state current of ~2.83 μA, and rising and falling times were measured as ~30 and ~16 ms, respectively, for 100 ms laser pulses.

©2015 Optical Society of America

OCIS codes: (160.6990) Transition-metal-doped materials; (250.6715) Switching; (140.3440) Laser-induced breakdown; (310.0310) Thin films.

References and links

1. F. J. Morin, "Oxides which show a metal-insulator transition at the Neel temperature," *Phys. Rev. Lett.* **3**(1), 34–36 (1959).
 2. N. F. Mott and L. Friedman, "Metal-insulator transitions in VO₂, Ti₂O₃ and Ti_{2-x}V_xO₃," *Philos. Mag.* **30**(2), 389–402 (1974).
 3. M. M. Qazilbash, M. Brehm, B.-G. Chae, P.-C. Ho, G. O. Andreev, B.-J. Kim, S. J. Yun, A. V. Balatsky, M. B. Maple, F. Keilmann, H.-T. Kim, and D. N. Basov, "Mott transition in VO₂ revealed by infrared spectroscopy and nano-imaging," *Science* **318**(5857), 1750–1753 (2007).
 4. E. Arcangeletti, L. Baldassarre, D. Di Castro, S. Lupi, L. Malavasi, C. Marini, A. Perucchi, and P. Postorino, "Evidence of a pressure-induced metallization process in monoclinic VO₂," *Phys. Rev. Lett.* **98**(19), 196406 (2007).
 5. A. Cavalleri, C. Tóth, C. W. Siders, J. A. Squier, F. Ráksi, P. Forget, and J. C. Kieffer, "Femtosecond structural dynamics in VO₂ during an ultrafast solid-solid phase transition," *Phys. Rev. Lett.* **87**(23), 237401 (2001).
 6. S. Han, C. H. Chun, C. S. Han, and S. M. Park, "Coupled physics analyses of VO_x-based, three-level microbolometer," *Electron. Mater. Lett.* **5**(2), 63–65 (2009).
 7. M. Rini, A. Cavalleri, R. W. Schoenlein, R. López, L. C. Feldman, R. F. Haglund, Jr., L. A. Boatner, and T. E. Haynes, "Photoinduced phase transition in VO₂ nanocrystals: ultrafast control of surface-plasmon resonance," *Opt. Lett.* **30**(5), 558–560 (2005).
 8. G. Stefanovich, A. Pergament, and D. Stefanovich, "Electrical switching and Mott transition in VO₂," *J. Phys. Condens. Matter* **12**(41), 8837–8845 (2000).
-

9. Y. W. Lee, B.-J. Kim, J.-W. Lim, S. J. Yun, S. Choi, B.-G. Chae, G. Kim, and H.-T. Kim, "Metal-insulator transition-induced electrical oscillation in vanadium dioxide thin film," *Appl. Phys. Lett.* **92**(16), 162903 (2008).
10. D. Ruzmetov, G. Gopalakrishnan, J. D. Deng, V. Narayanamurti, and S. Ramanathan, "Electrical triggering of metal-insulator transition in nanoscale vanadium oxide junctions," *J. Appl. Phys.* **106**(8), 083702 (2009).
11. S. Chen, H. Ma, X. Yi, T. Xiong, H. Wang, and C. Ke, "Smart VO₂ thin film for protection of sensitive infrared detectors from strong laser radiation," *Sens. Actuators, A* **115**(1), 28–31 (2004).
12. H. Wang, X. Yi, S. Chen, and X. Fu, "Fabrication of vanadium oxide micro-optical switches," *Sens. Actuators, A* **122**(1), 108–112 (2005).
13. Y. W. Lee, B.-J. Kim, S. Choi, H.-T. Kim, and G. Kim, "Photo-assisted electrical gating in a two-terminal device based on vanadium dioxide thin film," *Opt. Express* **15**(19), 12108–12113 (2007).
14. J. D. Ryckman, V. Diez-Blanco, J. Nag, R. E. Marvel, B. K. Choi, R. F. Haglund, Jr., and S. M. Weiss, "Photothermal optical modulation of ultra-compact hybrid Si-VO₂ ring resonators," *Opt. Express* **20**(12), 13215–13225 (2012).
15. J. D. Ryckman, K. A. Hallman, R. E. Marvel, R. F. Haglund, Jr., and S. M. Weiss, "Ultra-compact silicon photonic devices reconfigured by an optically induced semiconductor-to-metal transition," *Opt. Express* **21**(9), 10753–10763 (2013).
16. B. K. Ridley and T. B. Watkins, "The possibility of negative resistance effects in semiconductors," *Proc. Phys. Soc. Lond.* **78**(2), 293–304 (1961).
17. Y. W. Lee, B.-J. Kim, S. Choi, Y. W. Lee, and H.-T. Kim, "Enhanced photo-assisted electrical gating in vanadium dioxide based on saturation-induced gain modulation of erbium-doped fiber amplifier," *Opt. Express* **17**(22), 19605–19610 (2009).
18. C. Ko, S. Ramanathan, "Effect of ultraviolet irradiation on electrical resistance and phase transition characteristics of thin film vanadium oxide," *J. Appl. Phys.* **103**(10), 106104 (2008).
19. B.-J. Kim, G. Seo, and Y. W. Lee, "Bidirectional laser triggering of planar device based on vanadium dioxide thin film," *Opt. Express* **22**(8), 9016–9023 (2014).
20. M. G. Hur, T. Masaki, and D. H. Yoon, "Thermochromic properties of Sn, W co-doped VO₂ nanostructured thin film deposited by pulsed laser deposition," *J. Nanosci. Nanotechnol.* **14**(12), 8941–8945 (2014).
21. S. Zhang, M. A. Kats, Y. Cui, Y. Zhou, Y. Yao, S. Ramanathan, and F. Capasso, "Current-modulated optical properties of vanadium dioxide thin films in the phase transition region," *Appl. Phys. Lett.* **105**(21), 211104 (2014).
22. B.-J. Kim, Y. W. Lee, S. Choi, S. J. Yun, and H.-T. Kim, "VO₂ thin-film varistor based on metal-insulator transition," *IEEE Electron Device Lett.* **31**(1), 14–16 (2010).
23. G. Seo, B.-J. Kim, J. Choi, Y. W. Lee, and H.-T. Kim, "Direct current voltage bias effect on laser-induced switching bistability in VO₂-based device," *Appl. Phys. Express* **5**(10), 102201 (2012).
24. H. S. Choi, J. S. Ahn, J. H. Jung, T. W. Noh, and D. H. Kim, "Mid-infrared properties of a VO₂ film near the metal-insulator transition," *Phys. Rev. B Condens. Matter* **54**(7), 4621–4628 (1996).
25. Y. Zhou, X. Chen, C. Ko, Z. Yang, C. Mouli, and S. Ramanathan, "Voltage-triggered ultrafast phase transition in vanadium dioxide switches," *IEEE Electron Device Lett.* **34**(2), 220–222 (2013).
26. S. B. Lee, K. Kim, J. S. Oh, B. Kahng, and J. S. Lee, "Origin of variation in switching voltages in threshold-switching phenomena of VO₂ thin films," *Appl. Phys. Lett.* **102**(6), 063501 (2013).
27. D. Ruzmetov, K. T. Zawilski, S. D. Senanayake, V. Narayanamurti, and S. Ramanathan, "Infrared reflectance and photoemission spectroscopy studies across the phase transition boundary in thin film vanadium dioxide," *J. Phys. Condens. Matter* **20**(46), 465204 (2008).
28. S. Lu, L. Hou, and F. Gan, "Preparation and optical properties of phase-change VO₂ thin films," *J. Mater. Sci.* **28**(8), 2169–2177 (1993).
29. M. A. Kats, D. Sharma, J. Lin, P. Genevet, R. Blanchard, Z. Yang, M. M. Qazilbash, D. N. Basov, S. Ramanathan, and F. Capasso, "Ultra-thin perfect absorber employing a tunable phase change material," *Appl. Phys. Lett.* **101**(22), 221101 (2012).
30. B. S. Yilbas and S. Z. Shuja, "Heat transfer analysis of laser heated surfaces – conduction limited case," *Appl. Surf. Sci.* **108**(1), 167–175 (1997).
31. D. Brassard, S. Fourmaux, M. Jean-Jacques, J. C. Kieffer, and M. A. El Khakani, "Grain size effect on the semiconductor-metal phase transition characteristics of magnetron-sputtered VO₂ thin films," *Appl. Phys. Lett.* **87**(5), 051910 (2005).
32. H.-M. Jung and S. Um, "Thermo-electrical properties of composite semiconductor thin films composed of nanocrystalline graphene-vanadium oxides," *J. Nanosci. Nanotechnol.* **14**(12), 9051–9059 (2014).

1. Introduction

Vanadium dioxide (VO₂) thin films exhibit unique and reversible phase transition (PT) between an insulating state and a metallic state, which is induced by temperature [1–3], pressure [4], light [5–7], and so forth. This PT is a fascinating phenomenon that can provoke and support the development of novel electrical and optical devices such as electrical switches and oscillators [8–10], infrared detectors [11], thermally triggered optical switches [12], optically gated electrical switches [13], optical ring resonators [14], and silicon photonic

devices [15]. When metal electrodes are formed on a VO₂ thin film to fabricate a two-terminal planar device, electric field can also trigger the PT [8–10]. This field-induced PT in the VO₂-based device usually accompanies an abrupt current jump in its current-voltage (*I-V*) properties, caused by the negative differential resistance (NDR) of VO₂ [16], and this nonlinear current increase can be beneficially applied to electrical switching apparatuses. In particular, optical stimuli cast on the VO₂ device can modulate this strongly nonlinear *I-V* behavior temporarily [13,17] or permanently [18]. From 2007, photo-assisted electrical gating, or the photonic control of the device current, was attempted by incorporating a 1.55 μm laser illuminating the VO₂ film of a two-terminal VO₂-based planar device [13], and its threshold voltage, at which a current jump occurred during the field-induced PT, could be controlled by the proper adjustment of the illumination power [13,17]. Recently, the bidirectional laser triggering, which implies that the device current bidirectionally switches increasing or decreasing according to the switched state (on- or off-state) of the illumination laser, was reported by switching on or off a 1.55 μm laser diode (LD) illuminating a two-terminal VO₂ device [19]. This bidirectional current switching (increase or decrease) is based on the forward or reverse field-induced PT of VO₂, triggered by the onset or the cutoff of the laser illumination. In [19], the bidirectional laser triggering of up to 10 mA was implemented with rising and falling times of ~192 and ~320 ms, respectively, but a switching contrast between on- and off-state currents was only ~68.2, which stemmed from a high off-state current, and the break-over voltage was as low as ~10.2 V. For VO₂-based devices to reach the level of practical light-triggered thyristors, a variety of device parameters should be further improved including a switching contrast and a break-over voltage. In order to enhance a switching contrast and a break-over voltage by facilitating the triggering of the PT under a low off-state current, a CO₂ laser centered at ~10.6 μm, with which a vigorous photo-thermally induced PT was anticipated, was considered as an illumination laser for the bidirectional laser triggering in VO₂ for the first time. Here, we demonstrated bidirectional laser triggering in a two-terminal planar device fabricated with a highly resistive VO₂ thin film grown by a pulsed laser deposition (PLD) method by controlling the optical power of a CO₂ laser illuminating the device. The output beam of the CO₂ laser was focused by a beam focusing setup so that it directly illuminated the film surface. First, a bias voltage range enabling the bidirectional laser triggering was determined from the *I-V* characteristics of the fabricated device. The break-over voltage of the device was measured as large as ~294.8 V, which resulted from the high resistivity of insulating VO₂ grains comprising the thin film and the large electrode separation of the device. Then, to investigate the temporal variation of the bidirectional triggering operation of the device current, its transient responses were analyzed with respect to various pulse widths and repetition rates of the illumination laser. In the transient responses of the VO₂ device biased at ~4.8 V, stable bidirectional laser triggering between 0 and 20 mA was observed attaining a maximum switching contrast of ~7067 for 100 ms laser pulses with a repetition rate of up to 3 Hz. Considerably high switching contrast is largely attributed to a low off-state current obtained from the large electrode separation and the high resistivity VO₂ film. In particular, due to lower absorption of the tetragonal phase VO₂ film at ~10.6 μm compared with the 1.55 μm absorption, rising and falling times could be also reduced as ~30 and ~16 ms, respectively.

2. Experimental setup and device preparation

Figure 1 shows the schematic diagram of the experimental setup in which a CO₂ laser (Synrad FSVi30SAC) with a center wavelength of ~10.6 μm illuminates the VO₂ film for bidirectional laser triggering in a two-terminal planar VO₂-based device. The maximum output power of the laser was ~40.18 W, measured by an optical power meter (Ophir Nova II, 7Z02696). The output power of the laser whose pulse width is modulated with a fixed carrier frequency of 5 kHz is adjusted by varying the duty ratio of periodical pulses, and the actual irradiation time is determined by a product of the duty ratio and the high-state duration of a TTL signal of the

function generator (Tektronix AFG3021C) fed into the laser controller via the external trigger port. To prevent the laser irradiation power from exceeding the film damage threshold, it was regulated to a power level of ~ 5.37 W by adjusting the duty ratio as 9%. Typical rising and falling times of the laser are ~ 29 and ~ 83 μ s, respectively, when it operates at a repetition rate of 500 Hz and a duty ratio of 50%, resulting in a pulse width of 1 ms. The output beam of the laser is internally collimated by a built-in lens, and the $1/e^2$ beam diameter and the full-angle beam divergence are ~ 2.35 mm and ~ 7.0 mRad, respectively. The collimated beam propagates to a gold-coated line mirror (Thorlabs NB1-L01) at which its propagation path is changed when reflected. The damage threshold and reflectivity of the gold-coated line mirror are 4000 W/mm and $> 99\%$ at 10.6 μ m, respectively. The reflected beam is introduced into a plano-convex lens (Thorlabs LA7660-F), used for beam focusing. The clear aperture and the effective focal length of the plano-convex lens for beam focusing are $> 80\%$ and ~ 75.0 mm at 10.6 μ m, respectively. The output power from the plano-convex lens was measured as ~ 4.77 W. The focused beam from the plano-convex lens was launched into the film at normal incidence. The position of the VO₂ device was precisely manipulated using an xyz translation stage for the surface spot diameter to be ~ 500 μ m. The optical intensity at the film surface was evaluated as ~ 2429.3 W/cm² at an incident optical power of ~ 4.77 W.

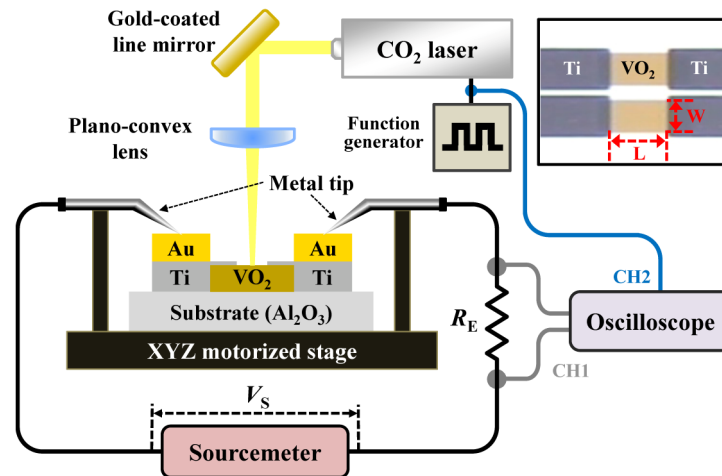


Fig. 1. Experimental setup for bidirectional laser triggering in two-terminal planar VO₂ device using CO₂ laser. The inset at an upper right corner shows the optical microscope image of the fabricated VO₂ device ($L = 100$ μ m and $W = 50$ μ m).

VO₂ thin films were grown on sapphire (Al₂O₃) substrates by a PLD method [20] for the fabrication of two-terminal planar devices. In order to decrease and increase the off-state current and the break-over voltage of the device, respectively, highly resistive VO₂ thin films were prepared by the minute control of an oxygen atmosphere (32 mTorr) and a substrate temperature (650 °C). The average thickness of the grown films was measured as ~ 100 nm. Au/Ti electrodes were formed on isolated VO₂ films, etched through ion beam-assisted milling technique, by a photolithographic method. Plane-view optical microscope images of fabricated devices are shown in the inset at an upper right corner of Fig. 1. The dimension of each device ($L \times W$) was 100×50 μ m², where L and W were the electrode separation length and exposed film width, respectively. Micromanipulators with metal tips were used on a probe station for forming electrical contacts with the fabricated device. To begin with, the electroforming of the contacts was performed to form a conducting path at the interface between the Ti electrode and the VO₂ film [21]. For the measurement of the transient responses of laser-triggered currents through the device, a test closed-loop circuit was constructed by combining a source meter (Keithley 2410), a VO₂ device, and a resistor with a

resistance of R_E , as shown in Fig. 1. The VO₂ device was connected in series with the sourcemeter and the resistor through metal tips. The sourcemeter was used as a voltage source for a DC bias V_S , which was applied to the circuit branch composed of the device and the resistor. The current flowing through the device was observed by monitoring the voltage across the resistor with an oscilloscope (Tektronix TDS2022C). To measure the I - V properties of the devices, only the sourcemeter was employed instead of the oscilloscope and resistor.

3. Results and discussion

Figure 2 shows the I - V characteristics of the fabricated VO₂ device, measured in a voltage-controlled mode (V-mode) with the CO₂ laser turned off and on, indicated as black circles and red triangles, respectively. As mentioned earlier, the laser illumination power was ~ 4.77 W when the laser was turned on. The compliance current was set as 20 mA to prevent excess current from flowing through the device. In case of the on state of the laser, the device resistance is reduced down to $(\sim 2.84 \text{ V})/(20 \text{ mA}) = \sim 142 \text{ } \Omega$ because most insulating VO₂ grains change into the metallic ones through the photo-thermally induced PT. The left inset of Fig. 2 shows the current-controlled mode (I-mode) I - V property of the device, measured without laser excitation. When the applied current flowing through the device exceeds a lower threshold current I_{TL} , measured as ~ 0.41 mA, the voltage across the device decreases from a higher threshold voltage V_{TH} , measured as ~ 294.8 V, showing an NDR characteristic. When the applied voltage exceeds V_{TH} (~ 294.8 V), the current flowing through the device abruptly jumps if measured in a V-mode, and the device resistance dramatically decreases. Thus, V_{TH} becomes the break-over voltage of the device. Although the I - V behavior of the device could not be measured with respect to the applied current > 0.5 mA due to the device breakage (indicated as a black dot) caused by high threshold voltage (compliance voltage = 300 V), the I - V trace of the device is expected to be a red dotted line for the applied current > 0.5 mA, when considering typical NDR properties of VO₂-based devices reported in many other works. The lower threshold voltage V_{TL} can be inferred as ~ 8.0 V from the laser-regulated current switching experiment which will be explained later. The right inset of Fig. 2 shows a resistance versus temperature curve of the VO₂-based device, and red circles and blue diamonds indicate heating and cooling curves, respectively. With the increase of temperature, the device resistance changes from ~ 1.92 M Ω at 25 °C to $\sim 133.5 \text{ } \Omega$ at 90 °C. The curves show that the PT occurs around 69 °C with a resistance variation of $\sim 1.44 \times 10^4$. The turn on resistance of the device obtained above ($\sim 142 \text{ } \Omega$), higher than the device resistance at 90 °C, indicates that there still exist insulating phases due to the conducting path of the filament at a device current of 20 mA, which leads to a device resistance larger than that measured thermally. When the device current is further increased by increasing the current compliance, all portions of VO₂ switch to the metallic phase by enough Joule heating [21,22].

If the VO₂ device is excited by the laser, the field-induced PT can easily occur even at low V_S due to the laser-induced drastic reduction of the device resistance. In case of the laser-induced PT based on a 1.55 μm laser, photo-excitation initially increases carriers in the VO₂ film at lower illumination powers, but carrier generation is dominated by the thermally induced PT at higher illumination powers [23]. Here, the photo-thermal effect of the CO₂ laser purely drives the PT and increases carriers because its photon energy is much smaller than the bandgap of VO₂ (~ 0.6 eV). The photo-thermally induced PT can be reversibly done by toggling the illumination laser unless the device temperature reaches a transition temperature of ~ 69 °C. For obtaining a high switching contrast through high off-state resistance, therefore, the device temperature should be maintained as low as room temperature, and the metal plate was attached to the backside of the device with thermally conductive adhesive for rapid heat dissipation. The energy per pulse (EPP), or the multiplication of the peak power and pulse width, and the repetition rate should be adequately balanced to achieve a high switching contrast, because the product of the EPP and the repetition rate determines the average power affecting the device temperature. Blue solid lines

shown in Fig. 2 show laser-regulated reversible current switching, i.e., the bidirectional current switching, which is measured at V_S increasing from 4.2 to 10.0 V with the laser arbitrarily turned on or off six times per state. The above V_S sweep was carried out for ~ 10 s, and the temporal interval between successive laser illuminations was > 0.5 s. In the V_S range of 4.2–7.6 V, five bidirectional laser triggering operations were achieved, and only a current increase was observed at the sixth operation with $V_S > 8.0$ V. It is found from these laser triggering operations that stable bidirectional current switching between 0 and 20 mA can be done by switching the laser on or off in the above V_S range from 4.2 to 7.6 V, but the device current jumped by laser excitation does not return to its off-state level even after the turn off of the laser at $V_S > 8.0$ V, that is, only unidirectional laser triggering is possible at $V_S > 8.0$ V.

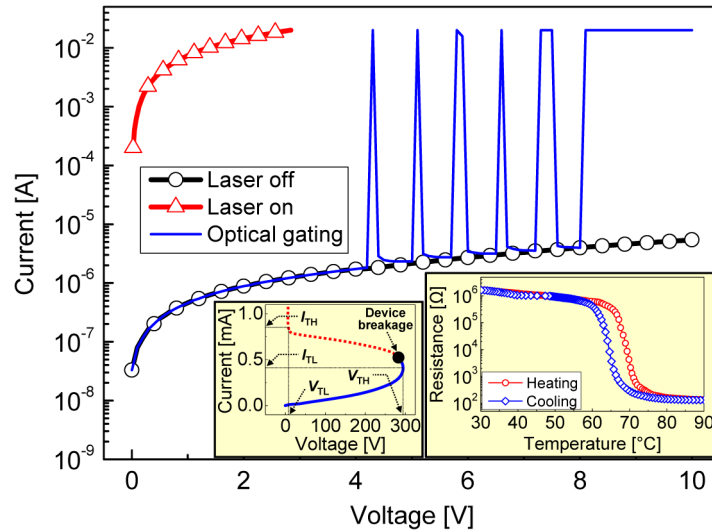


Fig. 2. I - V characteristics of fabricated VO_2 device, measured in V-mode with CO_2 laser switched on (red triangles) or off (black circles). Blue solid lines show laser-regulated reversible current switching. The left inset shows the I-mode I - V property of the device, measured without laser excitation. A black dot indicates the device breakage point. The right inset shows a resistance versus temperature curve of the device. Red circles and blue diamonds indicate heating and cooling curves, respectively.

In order to check the temperature increase caused by laser heating, the temperature variation at the laser spot was measured using a thermocouple in the first place when the CO_2 laser directly illuminated its sensor head with its surface beam diameter set as ~ 500 μm . The spot temperature was found to rise up to ~ 295.3 $^\circ\text{C}$ only 1 s after the 5 W illumination. The device temperature was also measured by attaching the sensor head of the thermocouple with silver paste to the surface of the device electrode adjacent to the laser irradiation point and was observed to increase by ~ 5.8 $^\circ\text{C}$ 1 s after the 5 W illumination. In our bidirectional laser triggering, the device temperature is not likely to significantly rise from room temperature and likely to find its equilibrium point less than the transition temperature of the fabricated VO_2 device, because the actual laser irradiation time is shorter than 1 s per pulse in transient response investigations for various pulse widths and repetition rates, which will be shown in Figs. 3 and 4. If the repetition rate increases over 3 Hz for 100 ms duration pulses, however, the device temperature is expected to gradually approach the transition temperature making off switching slow and ultimately impossible because the average power of the laser conveyed to the device is directly proportional to the repetition rate. In our laser-triggering experiments with a pulse width of 100 ms and a repetition rate < 3 Hz, although the device temperature is obviously lower than the transition temperature, VO_2 thin film in the device can be instantaneously changed into a metallic state when stimulated by the laser as the VO_2 active

area illuminated by the laser is as small as $100 \times 50 \mu\text{m}^2$, smaller than the beam spot diameter, and high optical absorbance ($> 80\%$) of a $\text{VO}_2/\text{Al}_2\text{O}_3$ structure at $10.6 \mu\text{m}$ [24]. Due to high absorption of the $\text{VO}_2/\text{Al}_2\text{O}_3$ structure, the laser energy is mostly converted to heat at the point at which absorption took place, and this converted heat energy facilitates the PT of VO_2 .

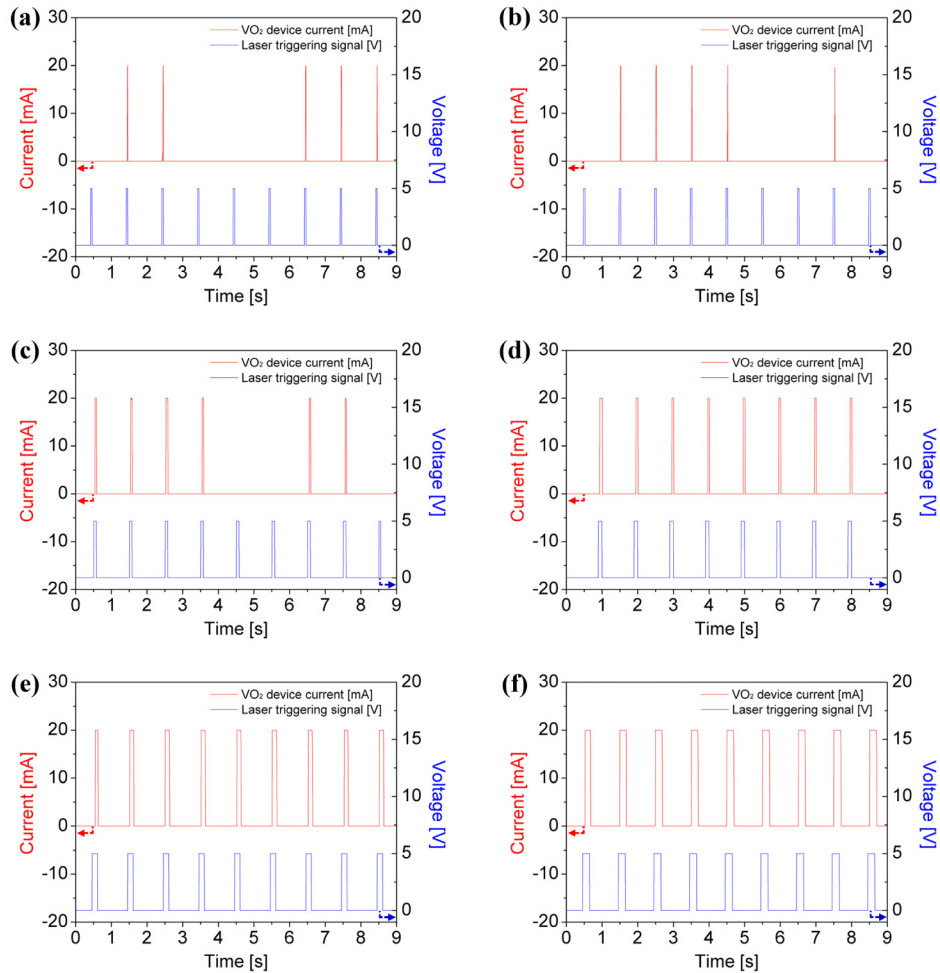


Fig. 3. Transient responses of laser-triggered device, measured for various on-state pulse widths such as (a) 40, (b) 50, (c) 75, (d) 100, (e) 150, and (f) 200 ms at a repetition rate of 1 Hz. The transient responses of the bidirectional laser triggering were examined in the circuit shown in Fig. 1 with $R_E = 100 \Omega$ and $V_S = \sim 4.8 \text{ V}$, and the compliance current was set as 20 mA.

Figures 3(a)-3(f) show the transient responses of the laser-triggered device when the laser whose illumination power from the plano-convex lens is $\sim 4.77 \text{ W}$ is modulated at a fixed repetition rate of 1.0 Hz with on-state pulse widths of 40, 50, 75, 100, 150, and 200 ms, respectively. The transient responses of the bidirectional laser triggering were measured in the test circuit shown in Fig. 1 with $R_E = 100 \Omega$ and $V_S = \sim 4.8 \text{ V}$, and the compliance current was set as 20 mA for all transient responses. As can be seen from Figs. 3(a)-3(c), the current switching operation is unstable and intermittent when the on-state pulse width is $< 100 \text{ ms}$. On the contrary, stable switching operations are observed when it exceeds 100 ms, as shown in Figs. 3(d)-3(f). From these results on the dependence of the bidirectional laser triggering on the on-state pulse width, the minimum EPP to sufficiently provoke the photo-thermally

induced PT can be determined as ~ 12.1 mJ by considering an on-state pulse width of 100 ms and the peak power delivered to the VO₂ film, which is calculated as ~ 121.4 mW from the product of the exposed film area (5×10^{-5} cm²) and the laser intensity (~ 2429.3 W/cm²). Although this result was drawn at a specific repetition rate (1 Hz), the same minimum EPP could be also obtained in slower repetition rates shown in Fig. 4 and especially in a single pulse. For EPPs less than the minimum EPP, the triggering operation is unstable and affected by ambient temperature, because the pulse energy is not enough to trigger the photo-thermally induced PT. If the spot size at the exposed film surface is further reduced by optimizing the beam focusing setup with additional lenses, the stable laser triggering operation is expected to be achieved for on-state pulse widths < 100 ms.

In order to investigate the dependence of the bidirectional laser triggering on the repetition rate of the laser, the laser output power from the plano-convex lens and the pulse width were set as ~ 4.77 W and 100 ms for satisfying the minimum EPP, and repetition rates were chosen as six different frequencies. Figures 4(a)-4(f) show the transient responses of the laser-triggered device, when the laser pulses with a 100 ms on-state pulse width are projected on the VO₂ device at repetition rates of 0.1, 0.2, 0.5, 1.0, 2.0, and 3.0 Hz, respectively. The test circuit used in Fig. 3 was employed again for the measurement with R_E and V_S kept as 100 Ω and ~ 4.8 V, respectively, and the compliance current was also set as 20 mA. It is found from Fig. 4 that stable bidirectional laser triggering of up to 20 mA is realized for a variety of repetition rates. The limitation of the repetition rate was 3 Hz, and it was observed that the falling time increased with the repetition rate over 3 Hz and a unidirectional switching occurred at a repetition rate of 4 Hz. This is because the average power of the laser conveyed to the device, affecting the device temperature, is directly proportional to the repetition rate. The increase of the device temperature slows off-switching responses increasing the falling time and ultimately makes the bidirectional switching impossible. If the beam intensity is further increased by reducing the spot diameter, laser pulses with shorter durations are expected to be able to trigger the PT of VO₂, and off-state durations without laser illumination become longer in a complementary manner, increasing the device cooling time. A prolonged device cooling time may increase the average power limit of the device and thus the repetition rate. The off-state current was measured as ~ 2.83 μ A, and the maximum switching contrast was evaluated as ~ 7067 . This switching contrast is 103 times higher than that obtained in our previous study [19], mainly attributed to a high room temperature absorbance of the VO₂ film on the Al₂O₃ substrate and a very low off-state current that originates from the large electrode separation of the device and the high resistivity of insulating VO₂ grains. The switching contrast obtained by the laser triggering is typically higher by more than 10 times compared with the voltage-induced triggering, because the device resistance change during the laser triggering nearly amounts to the resistance variation obtained during the structural PT [25]. But the voltage triggering is significantly superior to the laser triggering in the minimum triggering energy [25]. Regardless of the repetition rate, switching response times, i.e., rising and falling times, were measured as ~ 30 and ~ 16 ms, respectively, faster by more than 6 times the previous results [19]. Faster response times mainly come from the fast switching time of the modulated laser, relatively lower absorption of the metallic tetragonal VO₂ film on the Al₂O₃ substrate at ~ 10.6 μ m compared with that at ~ 1.5 μ m, and rapid heat dissipation by the metal plate attached to the backside of the device. The RC time constant of the test circuit can be approximately estimated to be on the order of $(100 \Omega) \times (100 \text{ pF}) = 10$ ns as the capacitance of the fabricated VO₂ device is on the order of 100 pF [9,26]. Although this RC time constant does not seem to affect the response time of the laser triggering, which is on the order of 10 ms, the increase of the external series resistance can delay the triggering response. It was also confirmed from additional experiments that there was no observable difference in the time dynamics of the laser-triggered VO₂ device for other external resistors with their resistance values $< 100 \Omega$. Reliability tests were also performed for 24 hours for the

experiments in Fig. 4, and no noticeable variation was found in the transient responses of laser-triggered currents.

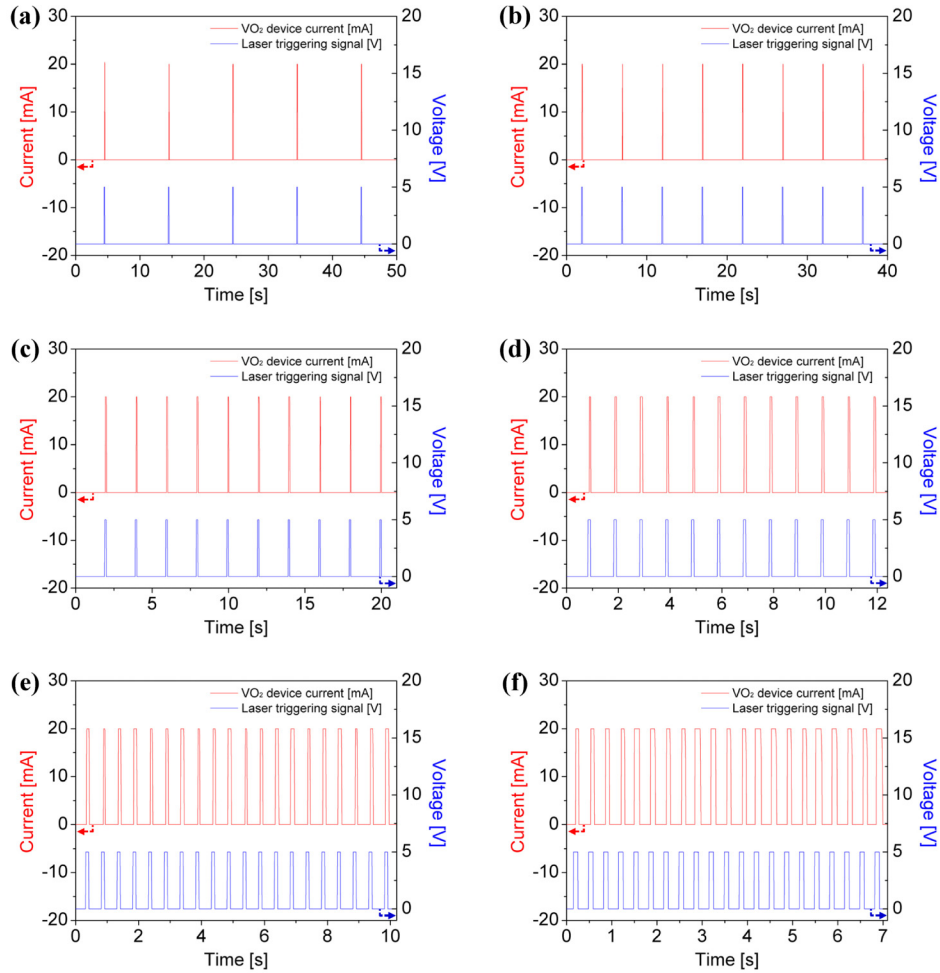


Fig. 4. Transient responses of laser-triggered device, measured for various repetition rates such as (a) 0.1, (b) 0.2, (c) 0.5, (d) 1.0, (e) 2.0, and (f) 3.0 Hz at a fixed pulse width of 100 ms. The same test circuit used in Fig. 3 was utilized for the measurement of the transient responses, and the compliance current was also set as 20 mA.

Considering the transmittance and the reflectance of VO₂ films grown on Al₂O₃ substrates reported in [24, 27], it can be inferred that the room temperature absorbance of the VO₂/Al₂O₃ structure at 10.6 μm becomes more than at least 80%. But, after the structural PT, this absorbance is severely reduced down to ~14% at 85 °C and can be further decreased down to < 7% at 120 °C [27]. In the case of a 1.55 μm LD, it can be inferred from [12,27,28] that the absorbance at 1.55 μm is quite small (< 10%) before the structural PT and fairly increases up to the level of 30% after the structural PT. As the room temperature absorption of the VO₂/Al₂O₃ structure is significantly higher at 10.6 μm compared with 1.55 μm, the use of a CO₂ laser rather than a 1.55 μm LD in the laser triggering can generate more heat in the VO₂ film at the same optical power and thus facilitate the complete structural PT (into a tetragonal phase) and the utilization of full resistance variation during the PT, resulting in a considerably improved switching contrast that is more than 100 times that obtained by the 1.55 μm LD [19]. Actually, in the previous study based on the 1.55 μm LD [19], all portions of the VO₂

film did not change into metallic tetragonal phases even at the maximum illumination power, as can be checked from nonlinear I - V curves shown in Fig. 2 of [19]. On the other hand, at high temperatures over the transition temperature of VO₂ (68 °C), the 10.6 μm absorbance of the VO₂/Al₂O₃ structure is relatively lower than the 1.55 μm absorbance as mentioned above. After the PT of the VO₂ film is triggered by a CO₂ laser, a low absorbance of < 10% is anticipated in the VO₂/Al₂O₃ structure because the laser may instantaneously raise the spot temperature up to > 80 °C. This low absorbance at 10.6 μm prevents the subsequent heating of the VO₂ film after the PT of the film is triggered, resulting in a faster falling time of the bidirectional laser triggering.

It is worthwhile to investigate how much the laser elevates the device temperature and what the minimum power to trigger the PT or to sustain the triggered state is by considering the photo-thermal effect of the laser and the heat dissipation effect in the device. For thermal analysis, a simple device structure, comprised of a VO₂ film on an Al₂O₃ substrate, two metal electrodes on both the film and the substrate, and a metal plate beneath the substrate, is considered. The heat generation and dissipative flow at the device structure can be classified into three stages: (1) The heat absorption of the VO₂ film on the substrate from incident infrared laser light, (2) the Joule heat created by the current flowing through the VO₂ channel after the PT of VO₂, and (3) the thermal dissipation through the substrate, the two electrodes, the metal plate, and the VO₂ film itself. At the first stage, the energy U_{VO_2} delivered to the film during an interval Δt is given by $U_{VO_2} = P_{IN}\Delta t\alpha(T)$ where P_{IN} is the incident laser power, and $\alpha(T)$ is the temperature-dependent absorbance of VO₂. Then, U_{VO_2} is calculated as $(\sim 121.4 \text{ mW}) \times (100 \text{ ms}) \times (\sim 0.8) = \sim 9.71 \text{ mJ}$, and it is assumed here that $\alpha(T)$ at room temperature is ~ 0.8 considering the transmittance and reflectance reported in [24,27,29]. At the second stage, the generated Joule heat, Q_{IV} , can be estimated by using electrical power P_{IV} consumed by the device for 100 ms, a pulse width of the laser. In the case of the bidirectional laser triggering ($V_s < 8 \text{ V}$), the Joule heat Q_{IV} generated in the VO₂ film becomes $(20 \text{ mA}) \times (\sim 2.84 \text{ V}) \times (100 \text{ ms}) = \sim 5.68 \text{ mJ}$, and this energy should be completely dissipated out of the film during 100 ms for the next triggering to happen. In the case of the unidirectional laser triggering ($V_s > 8 \text{ V}$), after the device is laser-triggered, the device current remains as 20 mA, and the voltage across the device is fixed as $\sim 8.0 \text{ V}$. The minimum power P_{min} , determined by the higher threshold current (I_{TH}) multiplied by $\sim 8.0 \text{ V}$, is required to sustain the triggered state. If the dissipation power is less than $(P_{IV} - P_{min})$, i.e., $(20 \text{ mA} - I_{TH}) \times (\sim 8.0 \text{ V})$, therefore, this unidirectional triggering can be maintained. That is, the dissipation energy Q_D for 100 ms should not be greater than $(20 \text{ mA} - I_{TH}) \times (\sim 8.0 \text{ V}) \times (100 \text{ ms})$, which is evaluated as $\sim 15.32 \text{ mJ}$ if I_{TH} is assumed as $\sim 0.85 \text{ mA}$. As the final stage, heat generated in the VO₂ film dissipates by conduction through the substrate, the metal plate attached to the substrate, two electrodes, and the film itself, which act as heat sinks.

If I_{TH} is assumed as $\sim 0.85 \text{ mA}$ in the following analysis, the actual heat dissipation energy Q_D from the device structure during 100 ms should be in the range from ~ 5.68 to $\sim 15.32 \text{ mJ}$ according to the above discussion on Q_D in both bidirectional and unidirectional triggering regions. If the residual heat energy Q_R , defined by subtracting Q_D from Q_{IV} , is smaller than the minimum energy for sustaining the triggered state, $I_{TH} \times (\sim 8.0 \text{ V}) = \sim 0.68 \text{ mJ}$, the bidirectional triggering is allowed at $V_s < 8 \text{ V}$. At $V_s > 8 \text{ V}$, the unidirectional triggering can be maintained if Q_R is larger than $\sim 0.68 \text{ mJ}$. In the laser triggering, Q_R for a 100 ms laser pulse can be estimated as $\sim 0.227 \text{ mJ}$ considering a laser pulse with a duration of $> 300 \text{ ms}$ inducing the unidirectional triggering. In order to check if this residual heat energy can trigger the PT of VO₂, a simple equation was adopted in [30] to calculate how much a CO₂ laser elevates the surface temperature of the VO₂ film. For a 100 ms laser pulse, the calculated surface temperature of the VO₂ film was $\sim 82.1 \text{ °C}$ with the assumption of the room temperature of 25 °C , which was higher than the transition temperature of the VO₂ device ($\sim 69 \text{ °C}$). Thermal constants of VO₂ such as a thermal conductivity of 3.6 W/m/K , a specific heat of 0.48876 J/g/K , and a density of 4.571 g/cm^3 were used in the calculation. The

dissipative heat energy Q_D can be also estimated by $U_{VO_2} - Q_R = \sim 9.483$ mJ. This estimated dissipation energy belongs to the predicted energy region of the actual heat dissipation.

Furthermore, the film thickness dependence of the device characteristics is well worth being considered. Typically, as the film thickness increases, the average grain size and resistance of the VO₂ film increases and decreases, respectively. The VO₂ grain size also influences directly on the amplitude and sharpness of the hysteresis curve in the thermally induced PT. With increasing grain size, which comes from thicker films, the density of grain boundaries and associated defects dwindle leading to stronger and sharper transition. On the contrary, the amplitude of the hysteresis curve decreases with decreasing film thickness [31], which may cause the reduction of the maximum on-state current and the switching contrast.

4. Conclusion

In summary, the bidirectional laser triggering was demonstrated in two-terminal planar devices based on highly resistive VO₂ thin films by utilizing the CO₂ laser centered at ~ 10.6 μm as an optical stimulus and harnessing the photo-thermally induced PT in VO₂. A bias voltage range for the stable operation of the bidirectional laser triggering was examined by incorporating the I - V properties of the VO₂ device. The bidirectional current switching of up to 20 mA was realized with a switching contrast of ~ 7067 by switching on or off the laser illuminating the VO₂ device biased at ~ 4.8 V. The switching contrast achieved here is 103 times higher than that obtained in the previous study. Through the investigation of the transient responses of laser-triggered currents, the minimum EPP at which the photo-thermally induced PT could be triggered was found to be ~ 12.1 mJ using laser pulses with a pulse width of 100 ms and a peak output power of ~ 4.77 W. With the laser pulse energy satisfying this minimum EPP, the bidirectional laser triggering was performed for a variety of repetition rates (0.1–3.0 Hz) with a fixed pulse width of 100 ms, and rising and falling times were measured as ~ 30 and ~ 16 ms, respectively. Large break-over voltages and high switching contrasts, implemented by the use of a CO₂ laser, may support the development of advanced laser-triggered oxide PT devices in future power electronics and electrical systems. Furthermore, photo-thermal triggering study in graphene-VO₂ films is anticipated to improve switching performances through the outstanding thermal characteristics of graphene [32].

Acknowledgments

This work was supported by the National Research Foundation of Korea(NRF) grant funded by the Korea government(MSIP) (No. 2013R1A2A2A01068390).